Volume 8
Number 9
September 2021
Pages 2345–2586

# Materials Horizons

rsc.li/materials-horizons

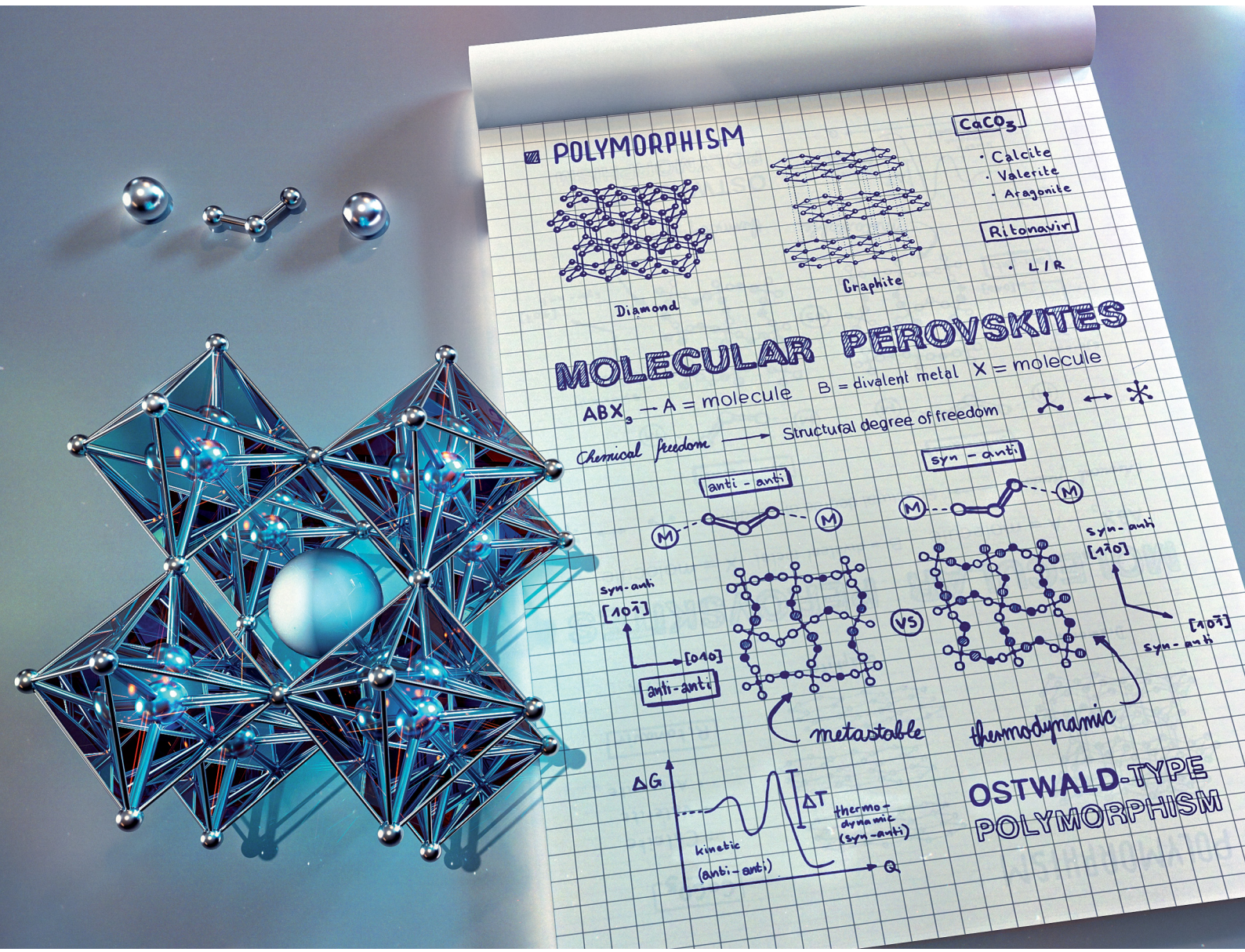


ISSN 2051-6347

ROYAL SOCIETY OF CHEMISTRY

**COMMUNICATION**
Ricardo Grau-Crespo, Gregor Kieslich *et al.*
Tilt and shift polymorphism in molecular perovskites

Materials Horizons

ROYAL SOCIETY OF CHEMISTRY

COMMUNICATION

View Article Online
View Journal | View Issue



Cite this: *Mater. Horiz.*, 2021, 8, 2444

Received 8th April 2021,
Accepted 14th June 2021

DOI: 10.1039/d1mh00578b

rsc.li/materials-horizons



# Tilt and shift polymorphism in molecular perovskites†

Stefan Burger, ‡[a] Shivani Grover,‡[b] Keith T. Butler, [c] Hanna L. B. Boström,[d] Ricardo Grau-Crespo *[b] and Gregor Kieslich *[a]

**Molecular perovskites, *i.e.* $ABX_3$ coordination polymers with a perovskite structure, are a chemically diverse material platform for studying fundamental and applied materials properties such as barocalorics and improper ferroelectrics. Compared to inorganic perovskites, the use of molecular ions on the A- and X-site of molecular perovskites leads to new geometric and structural degrees of freedom. In this work we introduce the concept of tilt and shift polymorphism, categorising irreversible perovskite-to-perovskite phase transitions in molecular perovskites. As a model example we study the new molecular perovskite series $[(n\mathrm{Pr})_3(CH_3)N]M(C_2N_3)_3$ with M = $Mn^{2+}$, $Co^{2+}$, $Ni^{2+}$, and *n*Pr = *n*-propyl, where different polymorphs crystallise in the perovskite structure but with different tilt systems depending on the synthetic conditions. Tilt and shift polymorphism is a direct ramification of the use of molecular building units in molecular perovskites and as such is unknown for inorganic perovskites. Given the role of polymorphism in materials science, medicine and mineralogy, and more generally the relation between physicochemical properties and structure, the concept introduced herein represents an important step in classifying the crystal chemistry of molecular perovskites and in maturing the field.**

### New concepts

Polymorphic phases often show different physicochemical properties, making polymorphism an important concept in the chemistry and physics of condensed matter. Some canonical examples that showcase the discipline crossing nature of polymorphism are the 1D and 3D form of $[(NH_2)_2CH]PbI_3$, the three different polymorphs of $CaCO_3$, and the different forms of ritonavir. In this work, the concept of tilt and shift polymorphism is introduced, categorising irreversible perovskite-to-perovskite phase transitions in the emerging material class of molecular perovskites. Molecular perovskites have recently gained attention in the field of ferroelectrics, multiferroics and mechanocalorics. The incorporation of molecular building blocks in the 3D $ReO_3$-type network of the perovskite structure leads to new geometric degrees of freedom, enabling the formation of polymorphic perovskite phases with different tilt and shift systems that are close in energy, *i.e.* tilt and shift polymorphs. Given the virtually unlimited chemical freedom to synthesise molecular perovskites of various kinds and the impact of structural details of the 3D network on the properties of molecular perovskites, tilt and shift polymorphism is an important new crystal chemistry principle.

## Introduction

Among dense coordination networks, the material class of $ABX_3$ coordination networks that crystallise in a perovskite structure holds a unique place.[1] Here referred to as molecular perovskites, the existence of a common building principle for a whole material class means that composition–structure–property relations can be studied in great depth.[2,3] Research on molecular perovskites can seek inspiration from the literature on inorganic perovskites, and in a subsequent step, investigate how the use of molecular building units leads to new crystal chemistry principles.[4] Therefore, molecular perovskites combine one of the most important structural motifs in condensed matter chemistry and physics with the nearly unlimited chemical diversity of coordination polymers—an exciting material platform in the search for phenomena of technological and scientific relevance such as barocalorics and improper ferroelectrics.[3,5–7]

Akin to inorganic perovskites, $ABX_3$ molecular perovskites show a 3D $[BX_3]^-$ network with **pcu** topology with the monovalent A-site cation sitting in the void of the network for charge balance.[8] The use of molecular X-site anions increases the size of the pseudocubic $ReO_3$-type network, so that molecular A-site cations

[a] *Department of Chemistry, Technical University of Munich, Lichtenbergstraße 4, 85748 Garching, Germany. E-mail: gregor.kieslich@tum.de*
[b] *Department of Chemistry, University of Reading, Whiteknights, Reading RG6 6DX, UK. E-mail: r.grau-crespo@reading.ac.uk*
[c] *Rutherford Appleton Laboratory, Scientific Computing Department (SciML), Didcot OX11 0QX, UK*
[d] *Max-Planck Institute for Solid State Research, Heisenbergstraße 1, 70569 Stuttgart, Germany*

† Electronic supplementary information (ESI) available: Details on experimental data as well as DFT calculations. CCDC 2068712, 2068716 and 2068842–2068849. For ESI and crystallographic data in CIF or other electronic format see DOI: 10.1039/d1mh00578b

‡ S. B. and S. G. contributed equally to this work and share first authorship.

with varying chemistries and sizes can be used to form molecular perovskites such as $[(NH_2)_3C]M(HCOO)_3$, $[(CH_3)_2NH_2]M(N_3)_3$, $[(C_2H_5)_3(C_7H_7)N]M(C_2N_3)_3$ and $[(Ph_3P)_2N]M[Au(CN)_2]_3$ with $M^{2+}$ typically being $Mn^{2+}$, $Co^{2+}$, $Ni^{2+}$ and $Zn^{2+}$.[9–14] More complex examples are the recently reported (defect-ordered) thiocyanate molecular perovskites,[15] A-site solid solutions,[16,17] molecular perovskites with mixed X-site anions,[18,19] and the conceptually related Prussian Blue Analogues.[20,21] The use of molecular moieties has important ramifications for the material properties, and formally, chemical (synthetic) freedom is translated to structural and geometric degrees of freedom.[22] For instance, molecular A-site cations enable temperature- and pressure-dependent order–disorder phase transitions related to the disorder of the molecular A-site cation,[23,24] and the integration of molecular X-site anions can lead to octahedral tilt patterns and columnar shifts that are intrinsically absent in inorganic perovskites.[25]

An important ramification of using molecular building units to form network materials is the introduction of weak chemical interactions such as dispersion interactions and hydrogen bonds. There are a number of research examples such as glass-type behaviour in $[(CH_3)_2NH_2]Zn(HCOO)_3$,[26] (defect-dependent) mechanical properties in $[(NH_2)_3C]Mn(HCOO)_3$,[27] temperature- and pressure-induced reversible ($[(CH_3)_2NH_2]M(HCOO)_3$)[28] and irreversible ($[(nPr)_4N]Cd(C_2N_3)_3$)[29] phase transitions, and more generally, structural distortions that can be activated by temperature and pressure, that all together point at relatively shallow free energy landscapes.[30] The recent discovery of irreversible phase transitions in the perovskite materials $[(NH_2)_3C]Mn(H_2POO)_3$, $[(C_5H_{10})_2N]Cd(C_2N_3)_3$ and $[(C_4H_9)_3(CH_3)N]Mn(C_2N_3)$ is in full agreement with this perspective.[31–33] For instance, crystal structure analysis for $[(NH_2)_3C]Mn(H_2POO)_3$ has shown that the different polymorphs are related to different tilt systems, *i.e.* the detailed distortion arrangement within the $[Mn(H_2POO)_3]^-$ network, reminiscent of conformational polymorphism as observed for molecular crystals.[34,35]

Considering the property-determining role of conformational polymorphism in molecular crystals,[36] knowledge and control of polymorphism in molecular perovskites is important in advancing the field, with a rigorous categorisation of this phenomenon representing the first step. Here we introduce the concept of *tilt and shift polymorphism* for molecular perovskites, studying its structural and thermodynamic origin. We report the new molecular perovskite series $[(nPr)_3(CH_3)N]M(C_2N_3)_3$ with M = $Mn^{2+}$, $Co^{2+}$, $Ni^{2+}$, *n*Pr = *n*-propyl and $C_2N_3^-$ = dicyanamide anion, which exhibits an irreversible perovskite-to-perovskite phase transition above room temperature. Depending on synthetic conditions, both polymorphs can be crystallised as single crystals. The series is used as a model example to establish the concept of tilt and shift polymorphism and to study its thermodynamic and structural nature by experiment and computation.

## Results and discussion

### Synthesis and structure determination

The series $[(C_3H_7)_3(CH_3)N]M(C_2N_3)_3$ with M = $Mn^{2+}$, $Co^{2+}$ and $Ni^{2+}$ was synthesised by applying an established mild-solution crystallisation route, where the precursor materials methyltripropylammonium chloride, sodium dicyanamide and the transition metal source were mixed at room temperature in an aqueous solution, see ESI,† for details. After two days, well-defined crystals suitable for single crystal X-ray diffraction formed. Within the series, all materials are isostructural and in the following discussion $[(C_3H_7)_3(CH_3)N]Ni(C_2N_3)_3$ is used as representative but the same conclusions can be drawn for $[(C_3H_7)_3(CH_3)N]Mn(C_2N_3)_3$ and $[(C_3H_7)_3(CH_3)N]Co(C_2N_3)_3$.

The structures of the as-synthesised materials were solved based on single-crystal X-ray diffraction (SCXRD) data recorded at 100 K. $[(C_3H_7)_3(CH_3)N]Ni(C_2N_3)_3$ crystallises in the orthorhombic space group *Pnma* with $a$ = 9.8624(6) Å, $b$ = 15.9509(9) Å and $c$ = 12.6923(7) Å, $V$ = 1996.7(2) Å$^3$. We refer to the as-synthesised polymorph as **P(Ni)-I**. The material crystallises in a perovskite structure where each dicyanamide linker coordinates two metal centres in a μ-1,5 fashion, spanning a three-dimensional $[Ni(C_2N_3)_3]^-$ coordination network with metal centres in an octahedral coordination. The molecular A-site cation $[(C_3H_7)_3(CH_3)N]^+$ sits in the void of the pseudocubic $[Ni(C_2N_3)_3]^-$ network for charge balance. Positional disorder is observed for the A-site cation $[(C_3H_7)_3(CH_3)N]^+$, with each propyl and methyl group disordered over two sites.

Subsequently, differential scanning calorimetry (DSC) was performed to screen for phase transitions (Fig. 1a). In the first heating cycle, a heat event at approximately $T$ = 365 K was observed. Given the absence of a corresponding signal in the cooling cycle, this is an irreversible event. Material change due to the loss of solvent molecules is excluded *via* thermogravimetric analysis coupled with mass spectrometry,[37] see ESI,† Fig. S4 and S5. Together with temperature-dependent powder X-ray diffraction which confirms crystallinity until material decomposition at $T$ > 530 K, Fig. S11 (ESI†), we can conclude that the heat event at $T$ = 365 K represents an irreversible crystalline-to-crystalline phase transition from polymorph **P(Ni)-I** into a material which is referred to as **P(Ni)-IIb**. Along the series $[(C_3H_7)_3(CH_3)N]M(C_2N_3)_3$ we find isostructural

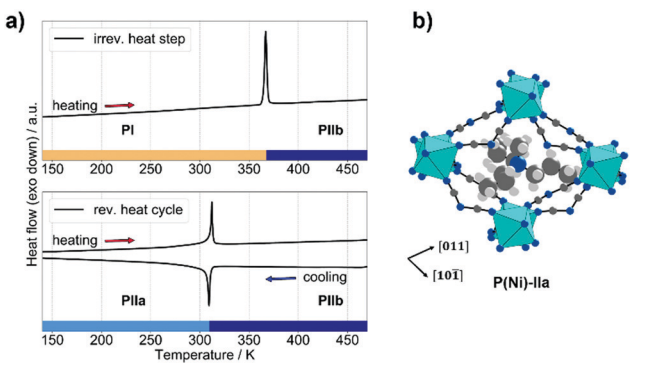


Fig. 1 (a) DSC traces of $[(nPr)_3(CH_3)N]Ni(C_2N_3)_3$. Shown are the heating step (top) and subsequent reversible cooling/heating cycle (bottom), highlighting the temperature range for the low-temperature and high-temperature phases with colour bars, respectively. (b) The pseudo-cubic coordination environment for the polymorph **P(Ni)-IIa**. Colour code: Ni – turquoise, N – dark blue, C – dark grey, H – light grey.

behaviour with increasing transition temperature from manganese to nickel, see Table S1 (ESI†) for an overview of thermodynamic parameters of the **P(M)-I**-to-**P(M)-IIb** phase transitions.

Such an irreversible phase transition was previously observed by us and others for $[(NH_2)_3C]Mn(H_2POO)_3$, $[(C_4H_9)_3(CH_3)N]Mn(C_2N_3)_3$ and $[(C_5H_{10})_2N]Cd(C_2N_3)_3$. For $[(NH_2)_3C]Mn(H_2POO)_3$, a single-crystal-to-single-crystal phase transition allowed for structure solution, showing an irreversible rearrangement of X-site molecules within the 3D $[Mn(H_2POO)_3]^-$ network as the underlying process.[31] Single crystals of **P(Ni)-I** break into a polycrystalline powder during the phase transition. To access structural details, we applied a high temperature crystallisation method at 370 K inspired by existing high-entropy nucleation routes.[38] After two days we obtained single crystals of **P(Ni)-IIb**, see ESI,† for experimental details. SCXRD at 350 K shows that **P(Ni)-IIb** adopts the perovskite structure motif, crystallising in the rhombohedral space group $R\bar{3}c$ with $a = b = 12.5350(3)$ Å, $c = 22.8074(12)$ Å and $V = 3103.52(19)$ Å$^3$. In **P(Ni)-IIb**, the A-site cation shows positional disorder, with all carbon atoms of the three propyl groups disordered over four positions and the methyl group disordered over two positions. Therefore, the phase transition from **P(Ni)-I** to **P(Ni)-IIb** represents an irreversible perovskite-to-perovskite phase transition. The two polymorphs **P(Ni)-I** and **P(Ni)-IIb** differ in the disorder of the A-site cation and, as will be established in the next section, in the chemical details of the tilt systems within the $ReO_3$-type network.

Following the traces of the DSC experiment, the irreversible heat event is followed by heat events that show the existence of a reversible phase transition. Therefore, **P(Ni)-IIb** represents a high-temperature phase of $[(C_3H_7)_3(CH_3)N]Ni(C_2N_3)_3$ with a reversible phase-transition to a low-temperature phase that we call **P(Ni)-IIa**, see Fig. 1a (bottom). SCXRD experiments at 100 K show that **P(Ni)-IIa** crystallises in the polar space group $R3c$ with $a = b = 12.5883(8)$ Å, $c = 21.5650(2)$ Å and $V = 2959.5(4)$ Å$^3$, see ESI,† for details. For **P(Ni)-IIa** we find a fully ordered A-site cation, showing that the reversible phase transition **P(Ni)-IIa** to **P(Ni)-IIb** is an order–disorder phase transition related to the A-site cation. Such polar-to-nonpolar phase transitions, where A-site disorder introduces inversion symmetry, are well known for molecular perovskites.[39,40] Looking at the material metal series, phase transition temperatures correlate with size and ligand field stabilisation energy (LFSE) of the divalent metal, *i.e.* $T_c$(**P(M)-IIa** to **P(M)-IIb**) = 284 K ($Mn^{2+}$), 301 K ($Co^{2+}$) and 312 K ($Ni^{2+}$). The reversible phase transition shows analogies to phase transitions in $[(C_3H_7)_4N]Mn(C_2N_3)_3$[41] and $[(C_3H_7)_4N]Cd(C_2N_3)_3$,[42] and thermodynamic data implies interesting barocaloric performances (Table S1, ESI†); however, such a characterisation goes beyond the scope of this work where the polymorphism between **P(Ni)-I** and **P(Ni)-II** is in the focus.

## Tilt and shift polymorphism

Now we analyse the details of the structural differences between the polymorphs **P(M)-I** and **P(M)-II**, with focus on the structural details of the 3D $[M(C_2N_3)_3]^-$ networks. The tilt distortions in

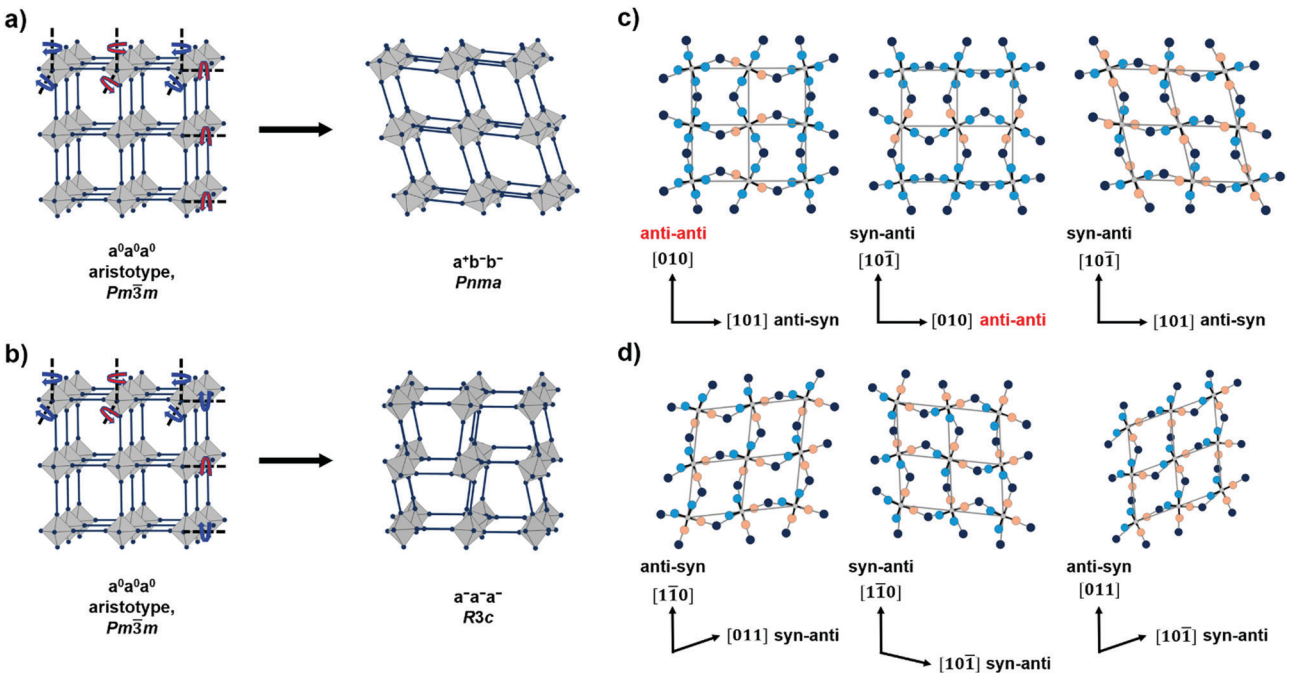


Fig. 2 (a and b) the tilt systems of the polymorphs **P(M)-I** and **P(M)-IIa** as derived from a hypothetical aristotype network with $Pm\bar{3}m$ symmetry (schematic is inspired from ref. 47). Red arrows indicate clockwise and blue arrows indicate *anti*-clockwise tilts of octahedra; (c and d) show 2D projections of the pseudocubic $ReO_3$-type network with emphasis on *syn–anti* and *anti–anti* binding modes of the metal–dicyanamide–metal network connectivity for **P(M)-I (c)** and **P(M)-IIa** (d). Colour code for dicyanamide in (c and d): central N – dark blue, terminal N *syn* – salmon, terminal N *anti* – light blue. Grey lines are a guide to the eye and do not represent chemical bonds.

 

both polymorphs can be described with the Glazer notation as established for inorganic perovskites,[40] see Fig. 2(a) and (b). The tilt pattern of the orthorhombic polymorph **P(M)-I** shows one in-phase and two out-of-phase tilts ($a^+b^-b^-$), while the rhombohedral polymorph only shows equilateral out-of-phase tilts ($a^-a^-a^-$). These tilt patterns and related space groups are common for inorganic oxide perovskites and molecular perovskites.[43–46]

When looking for the origin of these tilt patterns and a potential way to transform them into each other, a binding mode analysis of bonds between the multiatomic dicyanamide linker and the metal is required.[47] For a μ-1,5 coordination of the dicyanamide linker, three different binding modes are in principle possible: *syn–anti*, *syn–syn* and *anti–anti*.[48,49] For **P(M)-I** we observe binding modes that depend on the direction within the pseudocubic $[M(C_2N_3)_3]^-$ framework. Along $[10\bar{1}]$ and [101], a *syn–anti* connectivity is observed, while an *anti–anti* connectivity is found along [010]. In contrast, only *syn–anti* binding modes are found for the polymorph **P(M)-IIa**, see Fig. 2(c) and (d). Details on the assignment of *syn-* and *anti-*binding modes, including torsion angles, can be found in the ESI,† Table S9. Therefore, the irreversible phase transition from **P(M)-I** to **P(M)-II** is related to a change of binding modes from an *anti–anti* to *syn–anti* connectivity of the $[C_2N_3]^-$ anions, leaving the overall topology of the network unchanged. A change in X-site binding modes has been previously observed for the reversible pressure induced phase transition in $[(CH_3)_2NH_2]M(HCOO)_3$ (M = $Cu^{2+}$, $Fe^{2+}$ and $Mn^{2+}$) and an irreversible non-perovskite to perovskite phase transition is known for $[(n\mathrm{Pr})_4N]Cd(C_2N_3)_3$; however, the here presented $[(n\mathrm{Pr})_3(CH_3)N]M(C_2N_3)_3$ series combines both phenomena in a perovskite-to-perovskite irreversible phase transition related to a change in the binding mode.

A group-theoretical analysis of group–subgroup relations between the *Pnma* and $R\bar{3}c$ phases shows no obvious pathways for low-energy displacive phase transitions.[50] Any potential displacive phase transition would be expected to go through a high energy intermediate related to the aristotype in $Pm\bar{3}m$ which can be expected for a metastable phase. Across the metal series M = $Mn^{2+}$, $Co^{2+}$ and $Ni^{2+}$, we observe a monotonic increase of the phase transition temperatures from **P(M)-I** to **P(M)-IIb**, which agrees with the trend of decreasing metal ion radius (and increasing LFSE), see ESI,† Table S1 for details. In other words, the ligand-to-metal bond strength seems to play a role in the transformation mechanism from an *anti–anti* to *syn–anti* connectivity of the $(C_2N_3)^-$ X-site anions, arguably affecting the activation energy of the process. Since the network topology is maintained over the phase transition, describing this phase transition as 'reconstructive' seems inappropriate and a more detailed analysis is subject of future studies. Furthermore, we want to mention that the experimental, integrated phase transition enthalpies of this irreversible phase transition lie within the typical range,[51] but show no trends with metal radius, overall pointing towards a complex mechanism for the irreversible phase transition.

Following on from our results, and similar phenomena reported in the literature, we introduce the concept of tilt and shift polymorphism for molecular perovskites: tilt and shift polymorphism in molecular perovskites describes the existence of two molecular perovskites under the same conditions with the same composition, but with different underlying tilt systems and columnar shifts which may be transformed irreversibly into each other. While the presented examples only show Glazer-type (conventional) tilt polymorphism, we included the possibility of unconventional tilts and columnar shifts in this concept since preliminary results from us on $[(C_5H_{10})_2N]Cd(C_2N_3)_3$ show that this type of polymorphism potentially includes unconventional tilts and columnar shifts.[32] We want to emphasise that this definition involves the existence of at least one metastable molecular perovskite phase, and therefore excludes reversible perovskite-to-perovskite phase transitions as a function of temperature or pressure.[23,28,39]

As such, tilt and shift polymorphism of molecular perovskites is closely related to conformational polymorphism as known from molecular crystals.[35] Akin conformational polymorphism, the term 'tilt and shift polymorphism' is descriptive in nature. The origin of tilt and shift polymorphism is the variable binding mode of dicyanamide, and at the current state we can only speculate which factors bring different binding modes and the resulting molecular perovskites close in energy. We hypothesise that large A-site cations provide a larger configurational space for creating two distinct structures close in energy. Likewise, A-site cations with acidic H-atoms with the propensity for the formation of hydrogen bond networks seem beneficial.[28,30,31,52] The challenge in identifying such factors, which relates to the challenge to understand the interplay between A-site cation chemistry and the 3D network, brings us back to the task of engineering chemical interactions and therewith the underlying free energy landscape; an interdisciplinary challenge across various fields of condensed matter research.[53–55]

### Relative phase stabilities

To underpin experimental observations, we have used density functional theory (DFT) combined with lattice dynamic (LD) calculations, probing the relative stabilities of the different perovskite polymorphs. At 0 K, *i.e.* in the absence of any entropic contributions, a comparison of relative stabilities between rhombohedral and orthorhombic phases shows that the rhombohedral polymorph **P(M)-IIa** is the thermodynamically stable product when compared to **P(M)-I**, see Fig. 3a. Adding zero-point vibrational contributions to the energy difference reinforces the stability of the rhombohedral *vs.* the orthorhombic phase.

Since vibrational entropy can reverse thermodynamic stabilities at finite temperatures,[30,56,57] we calculated the vibrational free energy in the temperature range $T$ = 0–400 K for all **P(M)-I** and **P(M)-IIa** phases. We would like to note that phonon dispersion curves show some imaginary frequencies which are normally associated with dynamic instabilities; however, a

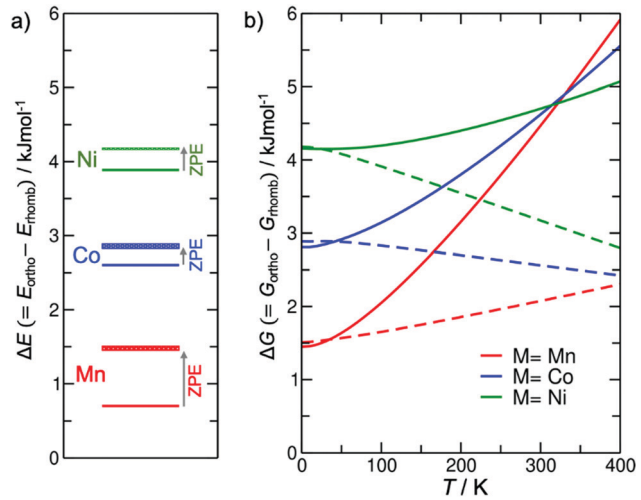


Fig. 3 (a) Energy differences between orthorhombic and rhombohedral phases for each composition, with and without zero-point energy (ZPE) corrections. (b) Vibrational free energy differences between the phases *vs.* temperature. The width of the ZPE-corrected lines in (a) and the two types of line in (b) reflect the different results from two ways of dealing with the (spurious) imaginary modes: ignoring the imaginary contributions (solid lines), or counting them as real contributions (dashed lines).

more in-depth analysis reveals that these imaginary frequencies are a numerical artefact from cell size effects for the LD simulations, see ESI.† In other words, both polymorphs are dynamically stable, and phase transitions between these phases are required to go through a high-energy intermediate rather than occurring *via* a simple displacive mechanism. Due to the spurious imaginary modes, which could not be re-normalised as we have done in previous studies,[58] we make two approximations for obtaining vibrational entropies: one to ignore the modes in the expression for free energy, the other to treat the negative modes as their positive inverse. These two approximations give extrema for how the free energy would evolve with temperature depending on the contribution of these modes. Fig. 3b shows unequivocally that the rhombohedral phase is more stable across the range of temperature of interest here, regardless of how we consider the contribution from the artificial imaginary modes. Therefore, we can here conclude that **P(M)-II** is the thermodynamically stable polymorph over the temperature range studied here, in excellent agreement with experimental observations, *i.e.* with the observation of crystallisation of this polymorph at higher temperatures.

Therefore, **P(M)-I** is the kinetic polymorph and its crystallisation seems to be kinetically favoured at ambient temperatures. Tilt and shift polymorphism for the here reported series $[(n\mathrm{Pr})_3(CH_3)N]M(C_2N_3)_3$ with M = $Mn^{2+}$, $Co^{2+}$, $Ni^{2+}$ is therefore of Ostwald type. Whilst currently known examples of molecular perovskites that show tilt and shift polymorphism such as $[(NH_2)_3C]Mn(H_2POO)_3$, $[(C_4H_9)_3(CH_3)N]Mn(C_2N_3)_3$ and $[(C_5H_{10})_2N]Cd(C_2N_3)_3$ all seem to fulfil the Ostwald-rule of phase occurrences, there is no fundamental reason why this rule must be fulfilled at all times; in other words, it is likely that other molecular perovskites exist where altering the synthetic conditions allows for obtaining tilt and shift polymorphism in molecular perovskites.

## Conclusion

In this work we introduce the concept of tilt and shift polymorphism for molecular perovskites, using the molecular perovskite series $[(n\mathrm{Pr})_3(CH_3)N]M(C_2N_3)_3$ with M = $Mn^{2+}$, $Co^{2+}$, $Ni^{2+}$ as a blueprint for establishing the concept. Depending on the synthetic conditions, different perovskite polymorphs are obtained, and thermal treatment of the metastable polymorph **P(M)-I** leads to an irreversible perovskite-to-perovskite phase transition to **P(M)-II**. The **P(M)-II** polymorph exhibits a reversible order–disorder phase transition (**PIIa–PIIb**), which shows promising characteristics in terms of barocaloric properties. In-depth analysis reveals that structural differences between polymorphs are related to a subtle but important difference of the binding modes within the 3D $[M(C_2N_3)_3]^-$ network, a mechanism intrinsically absent in inorganic perovskites. Density functional theory calculations show that for the whole stability temperature range the rhombohedral polymorph **P(M)-II** represents the thermodynamically more stable phase. The absence of real imaginary modes further suggests that the transformation goes through a high-energy transition state as underlying mechanism of the irreversible phase transition.

Tilt and shift polymorphism highlights the degrees of freedom, in this case, geometric degrees of freedom, that become accessible when moving from atomic to molecular building units. It underlines how little we have yet explored the vast chemical space of molecular perovskites, where subtle differences in the building principle can lead to different phases. The categorisation of tilt and shift polymorphism is important in developing the research area, helping us in the identification of degrees of freedom which have not yet been explored. When drawing comparisons to molecular crystals where properties such as optoelectronic properties and charge transport behaviour are tightly coupled to a distinct polymorph,[59,60] the necessity to understand and control tilt and shift polymorphism in molecular perovskites is apparent. For instance, the irreversible phase transition discussed here produces a molecular perovskite with promising phase transition thermodynamics for barocalorics, and the metastable form of $[(C_5H_{10})_2N]Cd(C_2N_3)_3$ crystallises in a polar space group with a large second harmonic generation. More generally, it is exciting to see how the use of chemically more complex building units stimulates research to develop new strategies and concepts for material analysis and interpretation, and as such, molecular perovskites present a fascinating material platform for research of academic and applied purposes.

## Author contributions

S. B. and G. K. designed the study. S. B. synthesised the samples and performed sample analysis. H. L. B. B. contributed with expertise on the tilt and shift system analysis. S. G., K. T. B. and

 

R. G. C. carried out the DFT calculations. S. B., S. G., K. T. B., R. G. C. and G. K. interpreted experimental and computational results, and wrote the manuscript with revision by all authors.

## Conflicts of interest

There are no conflicts to declare.

## Acknowledgements

S. B. is grateful for holding a doctoral scholarship from the Hanns-Seidel Foundation. GK would like to thank the Fonds der Chemischen Industrie for support through the Liebig Fellowship scheme. S. G. is grateful for a doctoral studentship from the Felix Trust. H. L. B. B. gratefully acknowledges financial support from the Alexander von Humboldt Foundation. S. B. thanks David C. Mayer and Christian Jandl for assistance and service for single-crystal X-ray diffraction measurements due to lab access restrictions during the Corona pandemic. This work made use of ARCHER, the UK's national high-performance computing service, *via* the UK's HPC Materials Chemistry Consortium, which is funded by EPSRC (EP/R029431), and of the Young supercomputer, *via* the UK's Materials and Molecular Modelling Hub, which is partially funded by EPSRC (EP/T022213/1).



## Notes and references

1 W. Li, Z. Wang, F. Deschler, S. Gao, R. H. Friend and A. K. Cheetham, *Nat. Rev. Mater.*, 2017, **2**, 16099.
2 W. Wei, W. Li, K. T. Butler, G. Feng, C. J. Howard, M. A. Carpenter, P. Lu, A. Walsh and A. K. Cheetham, *Angew. Chem., Int. Ed.*, 2018, **57**, 8932.
3 H. L. B. Boström, M. S. Senn and A. L. Goodwin, *Nat. Commun.*, 2018, **9**, 2380.
4 G. Kieslich and A. L. Goodwin, *Mater. Horiz.*, 2017, **4**, 362.
5 J. M. Bermúdez-García, M. Sánchez-Andújar and M. A. Señarís-Rodríguez, *J. Phys. Chem. Lett.*, 2017, **8**, 4419.
6 J. M. Bermúdez-García, M. Sánchez-Andújar, S. Castro-García, J. López-Beceiro, R. Artiaga and M. A. Señarís-Rodríguez, *Nat. Commun.*, 2017, **8**, 15715.
7 W.-J. Xu, Z.-Y. Du, W.-X. Zhang and X.-M. Chen, *CrystEngComm*, 2016, **18**, 7915.
8 S. Burger, M. G. Ehrenreich and G. Kieslich, *J. Mater. Chem. A*, 2018, **6**, 21785.
9 K.-L. Hu, M. Kurmoo, Z. Wang and S. Gao, *Chem. – Eur. J.*, 2009, **15**, 12050.
10 X.-H. Zhao, X.-C. Huang, S.-L. Zhang, D. Shao, H.-Y. Wei and X.-Y. Wang, *J. Am. Chem. Soc.*, 2013, **135**, 16006.
11 M.-L. Tong, J. Ru, Y.-M. Wu, X.-M. Chen, H.-C. Chang, K. Mochizuki and S. Kitagawa, *New J. Chem.*, 2003, **27**, 779.
12 J. Lefebvre, D. Chartrand and D. B. Leznoff, *Polyhedron*, 2007, **26**, 2189.
13 J. A. Hill, A. L. Thompson and A. L. Goodwin, *J. Am. Chem. Soc.*, 2016, **138**, 5886.
14 Z.-Y. Du, T.-T. Xu, B. Huang, Y.-J. Su, W. Xue, C.-T. He, W.-X. Zhang and X.-M. Chen, *Angew. Chem., Int. Ed.*, 2015, **54**, 914.
15 J. Y. Lee, S. Ling, S. P. Argent, M. S. Senn, L. Cañadillas-Delgado and M. J. Cliffe, *Chem. Sci.*, 2021, **9**, 2380.
16 S. Chen, R. Shang, B.-W. Wang, Z.-M. Wang and S. Gao, *Angew. Chem.*, 2015, **54**, 11093.
17 G. Kieslich, S. Kumagai, A. C. Forse, S. Sun, S. Henke, M. Yamashita, C. P. Grey and A. K. Cheetham, *Chem. Sci.*, 2016, **7**, 5108.
18 Y. Wu, D. M. Halat, F. Wei, T. Binford, I. D. Seymour, M. W. Gaultois, S. Shaker, J. Wang, C. P. Grey and A. K. Cheetham, *Chem. – Eur. J.*, 2018, **24**, 11309.
19 M. Mączka, A. Gągor, A. Pikul and D. Stefańska, *RSC Adv.*, 2020, **10**, 19020.
20 A. Simonov, T. de Baerdemaeker, H. L. B. Boström, M. L. Ríos Gómez, H. J. Gray, D. Chernyshov, A. Bosak, H.-B. Bürgi and A. L. Goodwin, *Nature*, 2020, **578**, 256.
21 A. E. Phillips and A. D. Fortes, *Angew. Chem., Int. Ed.*, 2017, **56**, 15950.
22 H. L. B. Boström and A. L. Goodwin, *Acc. Chem. Res.*, 2021, **54**, 1288.
23 W.-J. Xu, S.-L. Chen, Z.-T. Hu, R.-B. Lin, Y.-J. Su, W.-X. Zhang and X.-M. Chen, *Dalton Trans.*, 2016, **45**, 4224.
24 M. Mączka, I. E. Collings, F. F. Leite and W. Paraguassu, *Dalton Trans.*, 2019, **48**, 9072.
25 H. L. B. Boström, J. A. Hill and A. L. Goodwin, *Phys. Chem. Chem. Phys.*, 2016, **18**, 31881.
26 T. Besara, P. Jain, N. S. Dalal, P. L. Kuhns, A. P. Reyes, H. W. Kroto and A. K. Cheetham, *Proc. Natl. Acad. Sci. U. S. A.*, 2011, **108**, 6828.
27 H. L. B. Boström and G. Kieslich, *J. Phys. Chem. C*, 2021, **125**, 1467.
28 I. E. Collings, M. Bykov, E. Bykova, M. Hanfland, S. van Smaalen, L. Dubrovinsky and N. Dubrovinskaia, *CrystEngComm*, 2018, **20**, 3512.
29 M. Mączka, A. Gągor, M. Ptak, D. Stefańska and A. Sieradzki, *Phys. Chem. Chem. Phys.*, 2018, **20**, 29951.
30 G. Kieslich, S. Kumagai, K. T. Butler, T. Okamura, C. H. Hendon, S. Sun, M. Yamashita, A. Walsh and A. K. Cheetham, *Chem. Commun.*, 2015, **51**, 15538.
31 Y. Wu, S. Shaker, F. Brivio, R. Murugavel, P. D. Bristowe and A. K. Cheetham, *J. Am. Chem. Soc.*, 2017, **139**, 16999.
32 S. Burger, S. Kronawitter, H. L. B. Boström, J. K. Zaręba and G. Kieslich, *Dalton Trans.*, 2020, **49**, 10740.
33 M. Mączka, A. Gągor, M. Ptak, D. Stefańska, L. Macalik, A. Pikul and A. Sieradzki, *Dalton Trans.*, 2019, **48**, 13006.
34 J. Bernstein and A. T. Hagler, *J. Am. Chem. Soc.*, 1978, **100**, 673.
35 A. J. Cruz-Cabeza and J. Bernstein, *Chem. Rev.*, 2014, **114**, 2170.
36 A. Nangia, *Acc. Chem. Res.*, 2008, **41**, 595.
37 M. Mączka, A. Gągor, A. Stroppa, J. N. Gonçalves, J. K. Zaręba, D. Stefańska, A. Pikul, M. Drozd and A. Sieradzki, *J. Mater. Chem. C*, 2020, **8**, 11735.

38 S. Sobczak, P. Ratajczyk and A. S. Katrusiak, *Chem. – Eur. J.*, 2021, **27**, 7069.
39 M. Mączka, A. Gągor, M. Ptak, W. Paraguassu, T. A. da Silva, A. Sieradzki and A. Pikul, *Chem. Mater.*, 2017, **29**, 2264.
40 A. M. Glazer, *Acta Crystallogr., Sect. B: Struct. Crystallogr. Cryst. Chem.*, 1972, **28**, 3384.
41 J. M. Bermúdez-García, M. Sánchez-Andújar, S. Yáñez-Vilar, S. Castro-García, R. Artiaga, J. López-Beceiro, L. Botana, Á. Alegría and M. A. Señarís-Rodríguez, *Inorg. Chem.*, 2015, **54**, 11680.
42 J. M. Bermúdez-García, S. Yáñez-Vilar, A. García-Fernández, M. Sánchez-Andújar, S. Castro-García, J. López-Beceiro, R. Artiaga, M. Dilshad, X. Moya and M. A. Señarís-Rodríguez, *J. Mater. Chem. C*, 2018, **6**, 9867.
43 M. W. Lufaso and P. M. Woodward, *Acta Crystallogr., Sect. B: Struct. Sci.*, 2001, **57**, 725.
44 W. Li, Z. Zhang, E. G. Bithell, A. S. Batsanov, P. T. Barton, P. J. Saines, P. Jain, C. J. Howard, M. A. Carpenter and A. K. Cheetham, *Acta Mater.*, 2013, **61**, 4928.
45 P. Jain, V. Ramachandran, R. J. Clark, H. D. Zhou, B. H. Toby, N. S. Dalal, H. W. Kroto and A. K. Cheetham, *J. Am. Chem. Soc.*, 2009, **131**, 13625.
46 H. L. B. Boström, *CrystEngComm*, 2020, **22**, 961.
47 M. J. Cliffe, E. N. Keyzer, M. T. Dunstan, S. Ahmad, M. F. L. de Volder, F. Deschler, A. J. Morris and C. P. Grey, *Chem. Sci.*, 2019, **10**, 793.
48 X.-Y. Wang, Z.-M. Wang and S. Gao, *Chem. Commun.*, 2008, 281.
49 Z. Wang, K. Hu, S. Gao and H. Kobayashi, *Adv. Mater.*, 2010, **22**, 1526.
50 C. J. Howard and H. T. Stokes, *Acta Crystallogr., Sect. B: Struct. Sci.*, 1998, **54**, 782.
51 J. Nyman and G. M. Day, *CrystEngComm*, 2015, **17**, 5154.
52 I. E. Collings, R. S. Manna, A. A. Tsirlin, M. Bykov, E. Bykova, M. Hanfland, P. Gegenwart, S. van Smaalen, L. Dubrovinsky and N. Dubrovinskaia, *Phys. Chem. Chem. Phys.*, 2018, **20**, 24465.
53 A. P. Katsoulidis, D. Antypov, G. F. S. Whitehead, E. J. Carrington, D. J. Adams, N. G. Berry, G. R. Darling, M. S. Dyer and M. J. Rosseinsky, *Nature*, 2019, **565**, 213.
54 C. L. Hobday and G. Kieslich, *Dalton Trans.*, 2021, **50**, 3759.
55 A. D. Fortes, E. Suard and K. S. Knight, *Science*, 2011, **331**, 742.
56 K. T. Butler, P. Vervoorts, M. G. Ehrenreich, J. Armstrong, J. M. Skelton and G. Kieslich, *Chem. Mater.*, 2019, **31**, 8366.
57 K. T. Butler, K. Svane, G. Kieslich, A. K. Cheetham and A. Walsh, *Phys. Rev. B*, 2016, **94**, 180103.
58 G. Kieslich, J. M. Skelton, J. Armstrong, Y. Wu, F. Wei, K. L. Svane, A. Walsh and K. T. Butler, *Chem. Mater.*, 2018, **30**, 8782.
59 B. Huang, W.-C. Chen, Z. Li, J. Zhang, W. Zhao, Y. Feng, B. Z. Tang and C.-S. Lee, *Angew. Chem., Int. Ed.*, 2018, **57**, 12473.
60 T. Siegrist, C. Kloc, J. H. Schön, B. Batlogg, R. C. Haddon, S. Berg and G. A. Thomas, *Angew. Chem., Int. Ed.*, 2001, **40**, 1732.

 